Title	Chain dimensions and hydration behavior of collagen model peptides in aqueous solution: [Glycyl-4(R)-hydroxyprolyl-4(R)-hydroxyproline]n, [Glycylprolyl-4(R)-hydroxyproline]n, and some related model peptides
Author(s)	Terao, Ken; Mizuno, Kazunori; Murashima, Maiko et al.
Citation	Macromolecules. 2008, 41(19), p. 7203-7210
Version Type	AM
URL	https://hdl.handle.net/11094/81835
rights	This document is the Accepted Manuscript version of a Published Work that appeared in final form in Macromolecules, © American Chemical Society after peer review and technical editing by the publisher. To access the final edited and published work see https://doi.org/10.1021/ma800790w.
Note	

Chain Dimensions and Hydration Behavior of Collagen Model Peptides in Aqueous Solution: [Glycyl-4(*R*)-Hydroxyprolyl-4(*R*)-Hydroxyproline]*n*, [Glycyl-Prolyl-4(*R*)-Hydroxyproline]*n*, and Some Related Model Peptides

Ken Terao,[†],[*] Kazunori Mizuno,[‡],[§] Maiko Murashima,[†] Yusuke Kita,[†] Chizuru Hongo,[†] Kenji Okuyama,[†] Takashi Norisuye,[†] and Hans Peter Bächinger[‡],[§]

Department of Macromolecular Science, Osaka University, 1-1, Machikaneyama-cho, Toyonaka, Osaka, 560-0043, Japan, Department of Biochemistry and Molecular Biology, Oregon Health & Science University, Portland, Oregon 97239, and Research Department, Shriners Hospital for Children, Portland, Oregon 97239.

Running title: Dimensions and Hydration of Collagen Model Peptides in Solution
† Osaka University
‡ Oregon Health & Science University
§ Shriners Hospital for Children

ABSTRACT: Small-angle X-ray scattering (SAXS), circular dichroism (CD), and density measurements were made on eight samples of collagen model peptides consisting of glycine (Gly), proline (Pro), and 4-(*R*)-hydroxyproline (Hyp), i.e., (Gly-Hyp-Hyp)*n*, (Gly-Pro-Hyp)*n*, (Gly-Hyp-Pro)*n*, and (Gly-Pro-Pro)*n* (*n* = 5 and 9) in pure water and in phosphate buffered saline at a wide range of temperatures between 4 °C and 75 °C. A complete triple helical structure was found only for (Gly-Hyp-Hyp)$_9$ and (Gly-Pro-Hyp)$_9$ at 15 °C by SAXS and CD, and (Gly-Pro-Pro)$_9$ had a partially formed triple helix at 4°C. At 70 °C or higher temperatures, all peptides are dispersed as monomeric chains in these solvents and have essentially the same radii of gyration as the literature values for denatured proteins with the equivalent number of amino acid residues, suggesting that the conformational entropy for the single chain of the collagen model peptides is almost independent of the imino acid content. Furthermore, the partial specific volume $\bar{v}$ for (Gly-Hyp-Hyp)$_9$ around the transition temperature decreases more gradually with decreasing temperature than that for (Gly-Hyp-Hyp)$_5$. On the contrary, the temperature dependence of $\bar{v}$ for (Gly-Pro-Hyp)*n* has the opposite tendency, indicating that the hydration number for the peptide (Gly-Pro-Hyp)$_9$ increases with formation of the triple helix whereas that for the peptide (Gly-Hyp-Hyp)$_9$ decreases. These results are consistent with the difference in the transition enthalpies reported previously [*J. Biol. Chem.* 2004, *279*, 38072].

Introduction

Type I collagen, the most abundant structural protein in multicellular animals having a Gly-X-Y (Gly: glycine, X and Y are any amino residues) repeated sequence, has a different thermal stability for each organism and tissue. In fact, this temperature correlates strongly with the body temperature of the species.[1,2] The denaturation temperature is remarkably affected by the amino acid sequence and posttranslational modifications. However, it is very difficult to investigate the triple helix - coil transition precisely due to the complicated sequence of native collagens and the difficulty of complete renaturation *in vitro*. It was found several decades ago that the collagen model peptide (Gly-Pro-Pro)*n* (Pro: proline) shows a completely reversible conformational change between the single chain and the triple helix.[3] Furthermore, a 7/2-helical symmetry consisting of three peptide chains and more detailed structures were determined from the X-ray analysis of single crystals.[4,5,6] The average helical twists for many collagen model peptides were reported to be close to the ideal value for the 7/2 helix. The x-ray diffraction pattern from native collagen could also be explained by a 7/2-helical model.[7] This evidence

suggested that the triple helical structure of collagen model peptides is essentially the same as that of native collagens,[8] indicating that the collagen model peptides are a good model to investigate the triple helix-coil transition of collagen.

4-(R)-hydroxylation of proline residues in the Y position causes an extreme stabilization of the triple helix in aqueous media:[9,10,11,12] The triple helix consisting of $(Gly-Pro-Hyp)_n$ in solution unwinds at much higher temperature with a larger transition enthalpy than that of $(Gly-Pro-Pro)_n$.[13,14] This remarkable thermal stabilization has been at the center of controversial discussions about the stabilization of the collagen triple helix for years. On the one hand the stabilization is explained by water binding found in the crystal structure of collagen peptides,[15,16] mainly due to the water-mediated interchain hydrogen bonding. In fact, both the transition temperature and the enthalpy depend significantly on the position of hydroxyproline residue (X or Y) and the place of hydroxyl group on the pyrrolidine ring.[17,18,19] The effect of these water molecules observed in the crystal structures on the stability of the triple helical structure in solution is still not fully understood. The residency time of these water molecules was determined to be in the nanosecond to sub-nanosecond time range in solution by NMR[20] and direct water binding experiments showed only one water molecule bound per tripeptide unit, independent of the presence of Hyp.[13] The only direct water binding experiment was done in propanediol, which increases the transition temperature of the collagen model peptides. It is possible that the hydroxyl groups of the solvent can act as a mimic of bridged water molecules, however this is still an open question. For water binding to have an effect on the stability of the triple helix, a net increase in water binding upon structure formation is required. Kobayashi and colleagues[18,21] have reported the interaction of water with unfolded collagen-like chains and concluded that a high degree of hydration of $(Hyp-Hyp-Gly)_{10}$ in the single-coil state plays a key role in the thermal stability. The hydroxyl group of Hyp at the X position allows additional hydration in the single-coil state, resulting in a smaller enthalpy change than those of $(Pro-Hyp-Gly)_{10}$ and $(Pro-Pro-Gly)_{10}$. The smaller entropy change of $(Hyp-Hyp-Gly)_{10}$ is, in contrast, caused more significantly by the possible extensive hydration that restricts the mobility of water molecules.

The stabilizing effect of 4(R)-fluoroproline on the stability of the collagen triple helix points to an involvement of stereoelectronic effects in the determination of the stability.[19] The 4(R)-substitution by fluorine or hydroxyl groups has an effect on the proline ring puckering[22,23] and on the *cis/trans* ratio of the peptide bonds.[24] Because the collagen triple helix consists of all *trans* peptide bonds, the *cis/trans* ratio in the unfolded state directly effects the stability of the triple helix.

We[25] and Doi et al.[26] recently found that $(Gly-Hyp-Hyp)_n$ keeps the triple helical structure up to slightly higher temperature than that for $(Gly-Pro-Hyp)_n$ in aqueous solution whereas the transition enthalpy decreases to about half of the value of $(Gly-Pro-Hyp)_n$. Considering that the same helical symmetry with only a slight difference was observed for these two peptides,[21,27] it is quite unlikely that the difference is only due to the conformational entropy between these two triple helical structures; at least two more possible effects were therefore expected: 1. $(Gly-Hyp-Hyp)_n$ could have a lower conformational entropy than $(Gly-Pro-Hyp)_n$, 2. The hydration number could increase or decrease with the transition and the difference depends on the composition of the model peptides. The latter effect was suggested by Kawahara et al.[21] when comparing the partial specific volume $\bar{v}$ at two temperatures, that is, less than 10 °C and above 70 °C, ignoring however the normally pronounced temperature dependence of $\bar{v}$ without a transition. To decide between the above mentioned possibilities, the temperature dependence of $\bar{v}$ and the chain stiffness obtained from the radii of gyration and/or the particle scattering function were determined in the present work. The recent development of synchrotron radiation should allow us to detect small difference in dimensions even for relatively small biomolecules.

We prepared four different sequences of collagen model peptides $(Gly-Hyp-Hyp)_n$, $(Gly-Pro-Hyp)_n$, $(Gly-Hyp-Pro)_n$, and $(Gly-Pro-Pro)_n$ whose chemical structures are illustrated in Chart 1, and determined the radii of gyration and the particle scattering functions for those samples in aqueous media at 15 °C and 70 °C (or 75 °C). Different chain lengths ($n = 5$ and 9) were chosen for the present work because the helix-coil transition temperature depends generally on the number of residues due to the cooperative effect. The temperature dependence of $\bar{v}$ determined from density measurements allowed us to investigate the hydration effect on the conformational transition more precisely than by Kawahara et

al.[21] We note that pure water was also used as a solvent for some measurements to avoid preferential adsorption effect observed frequently for multi-component systems such as aqueous polymer solutions including some salt.

Experimental Section

Samples Preparation. Eight peptide samples, H-(Gly-Hyp-Hyp)$_n$-OH, H-(Gly-Pro-Hyp)$_n$-OH, H-(Gly-Hyp-Pro)$_n$-OH, and H-(Gly-Pro-Pro)$_n$-OH (n = 5, 9) were prepared using an ABI 433A synthesizer (Applied Biosystems, Foster City, CA); experimental details on synthesis, purification, and characterization are described elsewhere.[25] Lyophilized peptide samples were dissolved into pure water or 20 mM phosphate buffer, pH 7.0, containing 150 mM NaCl (PBS) at room temperature to prepare each test solution whose concentration was determined by weighing each component. The prepared solutions were stored at 4 °C until each measurement.

Circular Dichroism. Circular dichroism (CD) spectra for all investigated peptides in pure water and in PBS were recorded on a JASCO J720 spectropolarimeter (JASCO Instruments, Tokyo, Japan) in the range of wavelength λ_0 between 210 and 260 nm. A quartz cell with an optical path length of 2 mm was used and the temperature was controlled by use of a circulating waterbath. The scanning conditions were as follows: a bandwidth of 1.0 nm, a response time of 2 s, a scanning rate of 50 nm/min, and five times accumulations. The measurement for each solution was made at a concentration of (1-3)×10^{-4} g cm^{-3} from the lowest temperature and data acquisition at each temperature was begun about 10-30 minutes after the temperature of the cell holder had been stabilized. For the two peptides, (Gly-Hyp-Hyp)$_9$ and (Gly-Pro-Hyp)$_9$, temperature scans at 6 °C/h were recorded on an Aviv 202 spectropolarimeter (AVIV Biomedical, Inc., Lakewood, NJ) using a Peltier thermostated cell holder and a 1-mm path length rectangular quartz cell (Starna Cells Inc., Atascadero, CA).

Small-Angle X-ray Scattering (SAXS). Scattering intensities $I(k)$ at the absolute value of the scattering vector k for all peptide samples in pure water at 15 and 70 °C and in PBS at 15 and 75 °C filled in a 1.5 mmϕ quartz capillary were measured on a Rigaku R-AXIS IV++ imaging plate at the BL40B2 beamline in SPring-8 (Hyogo, Japan). The $I(k)$ data were corrected by the intensity of the direct beam detected both at the upper and lower ends of the capillary by ionic chambers. The wavelength, the camera length, and the accumulation time were set to be 0.10-0.15 nm, 1,000-1,500 mm, and 300 sec, respectively; the former two lengths correspond to the range of k less than 8 nm^{-1}. k at each pixel on the imaging plate was determined from the Bragg reflection of powdery lead stearate, and $I(k)$ at each k for solutions and solvents were determined by averaging the data whose scattering angle is essentially the same. The excess scattering intensity $\Delta I(k)$ was determined as the difference in $I(k)$ between the solution and the solvent. The apparent radius of gyration $<S^2>_{app}$ at finite solute mass concentration c was obtained from the Berry plot[28] on the basis of the following relationship

$$\left(\frac{c}{\Delta I(k)}\right)^{\frac{1}{2}} = \left(\frac{c}{\Delta I(0)}\right)^{\frac{1}{2}}\left[1 + \frac{1}{6}\left\langle S^2 \right\rangle_{app} k^2\right] \quad (1)$$

The mean-square radius of gyration $<S^2>$ was obtained by extrapolation of $<S^2>_{app}$ to infinite dilution, that is, $<S^2> = (<S^2>_{app})_{c\rightarrow 0}$. SAXS data were not taken for (Gly-Hyp-Pro)$_9$, (Gly-Pro-Pro)$_5$, and (Gly-Pro-Pro)$_9$ at 15 °C because some precipitates were observed in these solutions at room temperature.

Partial Specific Volume. The density ρ of the solvent and the solution was determined for all investigated model peptides with an Anton Paar DMA 5000 density meter to determine $\bar{v}$ at different temperatures. The following two methods were employed to confirm the reproducibility. (1) Conventional measurements were made for water and four solutions with different mass concentrations of 1-5×10^{-3} g cm^{-3} at 15, 35, 55, and 75 °C. Each data acquisition took about 30-40 minutes to equilibrate the solution density. (2) Programmed measurements for the solvent and a c of 5-10 × 10^{-3} g cm^{-3} were carried out from 75 °C to 4 °C, then 5 °C to 75 °C, with 1 °C interval. The average rate of

temperature change was 10-15 °C per hour.   The $\bar{v}$ data at each temperature was determined using the linear relation of $\rho = \rho_0 + (1-\bar{v}\rho_0)c$, where ρ_0 denotes the solvent density.

Results and Discussion

  Conformational Transition Temperature and Molar Mass of the Collagen Model Peptides.   It is well known that the CD spectra between 190 nm and 230 nm remarkably reflect higher order structures of polypeptides, e.g., α-helix, β-sheet, and multiple helices; for collagen and its model peptides, the conformational transition between the triple helix and the single chain can therefore be observed in the CD spectra around $\lambda_0 = 225$ nm.   Figure 1 illustrates typical CD spectra for our collagen model peptides consisting of 27 residues in PBS.   Most of the spectra have a maximum between 224 and 226 nm.   Temperature dependencies of the molar ellipticity $[\theta]$ at $\lambda_0 = 225$ nm are shown in Figure 2 for all peptide samples in PBS and for (Gly-Hyp-Hyp)$_n$ and (Gly-Pro-Hyp)$_n$ in pure water.   The data points for (Gly-Hyp-Hyp)$_5$ obey a straight line whose slope is about -25 deg cm^2 dmol^{-1} °C^{-1} irrespective of solvents as is the case with (Gly-Pro-Hyp)$_5$, (Gly-Hyp-Pro)$_5$, (Gly-Hyp-Pro)$_9$, and (Gly-Pro-Pro)$_5$, confirming that these four peptide samples do not form the triple helical structure in the temperature range investigated.   Although $[\theta]_{225}$ values for (Gly-Hyp-Pro)$_n$ are irrespective of the chain length, $[\theta]_{225}$ for (Gly-Hyp-Hyp)$_9$ and (Gly-Pro-Hyp)$_9$ in the two solvents have much larger values at 15 and 25 °C and decrease sharply between 25 and 55 °C toward those for (Gly-Hyp-Hyp)$_5$ and (Gly-Pro-Hyp)$_5$. This behavior suggests that (Gly-Hyp-Hyp)$_9$ and (Gly-Pro-Hyp)$_9$ form the triple helical structure in aqueous solution below 30 °C, unwind with increasing temperature, and disperse as a single peptide above 55 °C.   These transition temperatures are much lower than our previous data for longer peptides, Ac-(Gly-Hyp-Hyp)$_{10}$-NH$_2$ and Ac-(Gly-Pro-Hyp)$_{10}$-NH$_2$, due to the absence of both acetyl and amide end groups, low concentrations, and the shorter length of the peptides.   We also note that (Gly-Pro-Pro)$_9$ has only a slightly larger $[\theta]_{225}$ than those for (Gly-Pro-Pro)$_5$ [Figure 2(d)] below 20 °C due to the only partially formed triple helix. The two peptides that form a triple helix were further analyzed at a higher concentration with a slow temperature scanning rate (6 °C/h) [Figure 2(e)].   The transition temperature of (Gly-Pro-Hyp)$_9$ is 50.5 °C at a peptide concentration of 1.6 mM (3.9×10^{-3} g cm^{-3}), and the transition temperature of (Gly-Hyp-Hyp)$_9$ is 56.9 °C at a peptide concentration of 1.5 mM (3.9×10^{-3} g cm^{-3}).   The latter peptide has a 6.4 °C higher transition temperature.

  To confirm the triple helical structure in solution, the molar mass of the dispersed particle was measured by SAXS.   Figure 3 illustrates the square-root plots for (Gly-Hyp-Hyp)$_9$ and (Gly-Hyp-Hyp)$_5$ in pure water at 15 °C.   According to the scattering theory,[29] $\Delta I(0)/c$ (i.e., $\Delta I(k)/c$ at $k = 0$) is proportional to the product of the weight-average molar mass M_w of the solute and Δz^2 with Δz given by

$$\Delta z = z - \bar{v}\rho_{e,s} \qquad\qquad (2)$$

where z and $\rho_{e,s}$ are the number of moles of electrons per unit solute mass and the electron density of the solvent, respectively; the values of Δz have been determined in this study to be 0.173, 0.170, 0.157, and 0.153 mol g^{-1} for (Gly-Hyp-Hyp)$_5$, (Gly-Hyp-Hyp)$_9$, (Gly-Pro-Hyp)$_5$, and (Gly-Pro-Hyp)$_9$, respectively, in pure water at 15 °C.   Therefore, $\Delta I(0)$ is related to the M_w and the second virial coefficient A_2 by

$$\frac{Kc\Delta z^2}{\Delta I(0)} \equiv \frac{1}{M_{app}} = \frac{1}{M_w} + 2A_2 c + O(c^2) \qquad (3)$$

where M_{app} is the apparent molecular weight and K a constant for a given light source, capillary, and camera length. K was determined as the mean of the two independent estimates within 0.5% from the experimental $[c/\Delta I(0)]_{c\to 0}$ values for (Gly-Hyp-Hyp)$_5$ and (Gly-Pro-Hyp)$_5$ in water at 15 °C and their molecular weights based on the chemical structure.   With the acquired K value, M_w and A_2 were evaluated for (Gly-Hyp-Hyp)$_n$ and (Gly-Pro-Hyp)$_n$ in pure water at 15 °C from the concentration

dependence of $Kc\Delta z^2/\Delta I(0)$ shown in Figure 4 and the resultant values are summarized in Table 1 along with the calculated molecular weights M. The M_w values for the longer peptides are about three times larger than the corresponding M values, indicating that (Gly-Hyp-Hyp)$_9$ and (Gly-Pro-Hyp)$_9$ are dispersed as triple helices in solution.

We determined A_2 for the peptides in PBS solution (Table II) from the intercepts J and slopes S of the $c/\Delta I(0)$ against c plots according to the relation

$$A_2 = \frac{S}{2JM_w} \qquad (4)$$

instead of eq 3. Application of eq 3 was impossible because it was not feasible to determine $\bar{v}$ for dialyzed solutions of lower molar mass multi-component systems. For M_w in eq 4, we used $3M$ for the triple-helical (Gly-Hyp-Hyp)$_9$ and (Gly-Pro-Hyp)$_9$ at 15 °C and M for all other peptides. The resultant A_2 values are plotted against temperature in Figure 5. Interestingly, A_2M_w data for the triple helix at 15 °C have positive values reflecting a good solubility in both water and PBS, whereas those for single chains at the same temperature are less than zero. In contrast, those at 75 °C are positive and close to each other. The change in A_2 from negative to positive values with increasing temperature for single chains shows that the interaction between peptide molecules changes from attractive to repulsive. Furthermore, positive A_2 values for triple helices at 15 °C also indicate that the sites having attractive interactions among single peptides at 15 °C disappear with formation of the triple helix. In other words, the monomeric collagen-like peptides have a tendency to interact with each other even though they are not long enough to form a stable triple helix, but after the formation of the triple helix, the molecules show repulsive interactions. This temperature and conformation-dependent behavior of the peptide-peptide interaction probably directly relates to the conformational transition behavior of collagen model peptides. The following experimental fact supports this hypothesis. H-(Gly-Hyp-Pro)$_5$-OH has a positive A_2 at 15 °C, as shown in Figure 5 and Table 1, while its longer peptide, that is, H-(Gly-Hyp-Pro)$_9$-OH, does not form a triple helical structure in solution even at 15 °C.

Dimensional Properties. *Triple Helices in Solution.* As clearly seen in Figure 6, $<S^2>^{1/2}$'s for the triple-helical collagen model peptides (triangles), plotted against the number of residues, are about 1.6 times larger than those for single molecules due to the rodlike nature of the triple helices. The $<S^2>^{1/2}$ values of 2.3-2.4 nm for the triple helices listed in Tables 1 and 2 correspond to the total contour length of 8.0-8.3 nm along the helix axis, which essentially agrees with the distance 8.15 nm of the furthest COOH and NH$_2$ groups in the crystal structure of (Gly-Hyp-Hyp)$_9$. Holtzer plots[30] of $kP(k)$ vs. k for the triple helices show no clear plateau as illustrated in Figure 7 because of the relatively low axial ratios, where $P(k)$ is the particle scattering function defined by $\Delta I(k)/\Delta I(0)$ at infinite dilution. The solid curves in the figure have been calculated for the straight cylinders with the indicated values of the length L and diameter d using the following approximate expression:[31,32]

$$P(k) = \frac{2kL\,\mathrm{Si}(kL) + 2\cos(kL) - 2}{(kL)^2} \left[\frac{2J_1(kd/2)}{kd/2} \right]^2 \qquad (5)$$

These curves fit the data points for the respective peptides only in the range of $k < 1.5$ nm^{-1}, though the $<S^2>^{1/2}$ values calculated by $<S^2> = L^2/12 + d^2/8$ with the same parameters agree almost perfectly with the experimental ones listed in Table 2. The discrepancy between the experimental and theoretical $P(k)$ in the higher k range may reflect effects of the local atomic positions and hydration water molecules. Indeed, $P(k)$ for the atomic coordinate of (Gly-Hyp-Hyp)$_9$[27] obtained from the protein data bank (1YM8) (the dashed curve in Figure 7) closely fits the experimental data points when computed with the program CRYSOL[33] by taking into account the influence of the hydration shell. These findings demonstrate that the triple-helical structure of the model peptides in the single crystal is maintained in solution.

Single Model Peptide Chains in Solution. Figure 6 indicates that $\langle S^2\rangle^{1/2}$'s for the single peptide chains are essentially identical with the known data for chemically unfolded globular proteins[34] having much fewer imino acids in the sequence. The restriction of the internal rotation does not cause a significant increase in $\langle S^2\rangle^{1/2}$ in aqueous solution. Alternatively, this restriction at each imino acid residue would be compensated by the flexible glycyl bonds and the increased propensity for *cis* Pro/Hyp bonds, resulting in an average $\langle S^2\rangle^{1/2}$. These findings are in agreement with the Tiffany and Krimm model, which indicates that unfolded chains of globular proteins consist of short stretches of polyproline II-like structures, regardless of the amino acid sequence.[35,36,37]

If single collagen-like peptide chains are modeled by the unperturbed wormlike chain with finite thickness, their statistical properties are determined by L (the contour length), λ^{-1} (the Kuhn segment length), and d. The first parameter is related to h (the contour length per amino acid residue) and the number N of amino acid residues per molecule by $L = Nh$. The last parameter may approximately be estimated for rather flexible wormlike chains using the cross-sectional plot [$\ln kP(k)$ vs k^2][29,32] as illustrated in Figure 8 for the model peptides in PBS at 75 °C. The indicated straight lines fitting the data points in the range of k^2 between 5 and 15 nm^{-2} yield the values of d^2 shown in the figure. These d^2 values are only apparent, and the anomalous, negative d^2 for (Gly-Pro-Pro)$_n$ may be regarded as due to the distribution of the cross-sectional electron density.[38]

With use of the apparent d^2 values, we evaluated a set of h and λ^{-1} for each (Gly-X-Y)$_n$ in PBS at 75 °C from the $\langle S^2\rangle$ data (for $n = 5$ and 9) by numerically solving the equation[39,40]

$$\langle S^2\rangle = \frac{L}{6\lambda} - \frac{1}{4\lambda^2} + \frac{1}{4\lambda^3 L} - \frac{1}{8\lambda^4 L^2}\left[1 - \exp(-2\lambda L)\right] + \frac{d^2}{8} \tag{6}$$

with the result that $h = 0.32\text{-}0.34$ nm and $\lambda^{-1} = 1.9\text{-}2.3$ nm; we note that the contribution of the last term $d^2/8$ to $\langle S^2\rangle$ was only 5.2% even for $n = 5$. Considering a possible experimental error ($\pm 2\%$) in $\langle S^2\rangle$ causes errors of ± 0.05 nm and ± 0.7 nm for h and λ^{-1}, respectively, we may conclude that the collagen-model peptides have $h = 0.33 \pm 0.06$ nm and $\lambda^{-1} = 2 \pm 1$ nm almost irrespective of their sequence. The solid curves in Figure 9, computed from Nakamura and Norisuye's theory[32] for the wormlike cylinder model, show that these parameters allow the k-dependence of experimental $kP(k)$ to be explained in the range of $k < 3.5$ nm^{-1} when the (apparent) d is chosen to be 0, 0.45, 0.45, and 0.67 nm for (Gly-Pro-Pro)$_n$, (Gly-Hyp-Pro)$_n$, (Gly-Pro-Hyp)$_n$, and (Gly-Hyp-Hyp)$_n$, respectively (see the d^2 values in Figure 8). We found that the above procedure leads to substantially the same h and λ^{-1} values in pure water as those in PBS (not shown here).

In order to explain the small transition enthalpy and entropy of the peptide Ac-(Gly-Hyp-Hyp)$_{10}$-NH$_2$ compared to that of the peptide Ac-(Gly-Pro-Hyp)$_{10}$-NH$_2$, we proposed that the unfolded state of the peptide (Gly-Hyp-Hyp)$_n$ might be bridged by water molecules via the Xaa position 4-OH groups with the carbonyl group of the Yaa position Hyp, because when we observe a single chain from the crystal structure of the triple helix of the peptide H-(Gly-Hyp-Hyp)$_9$-OH, the water molecules can connect these intrachain groups.[27] If some 4-(R)-hydroxyl groups in a (Gly-Hyp-Hyp)$_n$ chain in solution are bridged through a water molecule, the internal rotation of the peptide chains could be restricted and may extend the main chain. The above mentioned analysis of $\langle S^2\rangle$ and $P(k)$ shows, however, that the intrachain hydrogen bonding through water molecules does not substantially affect the statistically-averaged chain dimensions of the peptide chains investigated. In other words, the hydrogen bonding may not exist or may be too weak to detect as the chain extension of the (Gly-Hyp-Hyp)$_n$ peptides in the unfolded state (75 °C). Our finding on $\langle S^2\rangle^{1/2}$ is also supported by the finding of Clerk and Mattice[41] that no significant difference in the intrinsic viscosity in water was detected between poly(Hyp) and poly(Pro) with the same weight-average molecular weight, although the measurements were made at 30 °C.

Hydration Effect on the Conformational Change: Partial Specific Volume. If the hydration number is affected by the peptide conformation, $\bar{v}$ can increase or decrease with the change in the conformation. Kawahara et al.[21] investigated $\bar{v}$ for (Hyp-Hyp-Gly)$_{10}$ and (Pro-Hyp-Gly)$_{10}$ in water

containing 100 mM acetic acid and found that the change in $\bar{v}$ for (Hyp-Hyp-Gly)$_{10}$ between 80 °C (single chain) and 10 °C (triple helix) was 3.0% whereas that for (Pro-Hyp-Gly)$_{10}$ was 8.2%. The latter value is much larger than the former one, and the authors concluded that the degree of hydration of (Hyp-Hyp-Gly)$_{10}$ is comparable to that of (Pro-Hyp-Gly)$_{10}$ in the triple-helical state, but the (Hyp-Hyp-Gly)$_{10}$ is more highly hydrated than (Pro-Hyp-Gly)$_{10}$ in the monomer state. This consideration is correct if the ratios of $\bar{v}_{80°C}$ to $\bar{v}_{10°C}$ are essentially the same for all investigated peptide samples; however no experimental evidence was shown for that. To clarify this point, (Gly-Hyp-Hyp)$_5$ and (Gly-Pro-Hyp)$_5$ are a good reference with no temperature induced conformational transition in aqueous solution.

The temperature dependences of $\bar{v}$ for (Gly-Hyp-Hyp)$_5$ and (Gly-Pro-Hyp)$_5$ in pure water are illustrated in Figure 10(a) along with those for (Gly-Hyp-Hyp)$_9$ and (Gly-Pro-Hyp)$_9$. Data points measured by increasing the temperature are almost the same as those measured by decreasing the temperature, indicating that equilibrium values were evaluated. We can detect a small difference even at 75 °C for filled and open symbols for $n = 9$ and 5, respectively. This difference is comparable with larger and smaller symbols obtained from independent measurements for the same systems, that is ±0.5% in $\bar{v}$, due to the possible error in solution preparation. Therefore, to compare $\bar{v}$ data changing with formation of or unwinding of the triple helix for these peptides, $\bar{v}_T/\bar{v}_{75°C}$ is plotted against the temperature in the panel (b) of Figure 10, where $\bar{v}_T$ and $\bar{v}_{75°C}$ are $\bar{v}$ at the temperature T and 75 °C, respectively; we note that the possible experimental error in $\bar{v}_T/\bar{v}_{75°C}$ is within ±0.2% because $\rho - \rho_0$ for the programmed measurements is greater than 1.5×10^{-3} g cm^{-3} and accurate to $\pm 3 \times 10^{-6}$ g cm^{-3}. $\bar{v}_T/\bar{v}_{75°C}$ for (Gly-Hyp-Hyp)$_9$ at the transition temperature has a smaller slope than that for (Gly-Hyp-Hyp)$_5$ whereas that for (Gly-Pro-Hyp)$_9$ has a larger slope; note that $\bar{v}_T/\bar{v}_{75°C}$ for (Gly-Hyp-Hyp)$_5$ are almost the same as that for (Gly-Pro-Hyp)$_5$. Given the almost equivalent triple helical structure for the two peptides both in solution [Figure 7] and single crystal,[21,27] the difference in $\bar{v}_T/\bar{v}_{75°C}$ may be due to the hydration behavior of the single chain. The result for (Gly-Pro-Hyp)$_9$ therefore indicates that the quantity of water molecules confining or strongly hydrogen bonded to the triple helices increases with forming a triple helix. On the contrary, such water molecules decrease for (Gly-Hyp-Hyp)$_9$. This finding can explain in part the experimental fact described above, that is, (Gly-Hyp-Hyp)$_9$ has higher thermal stability and much smaller transition enthalpy than (Gly-Pro-Hyp)$_9$ due to the great difference in the transition entropy. We note that the difference seen in $\bar{v}_T/\bar{v}_{75°C}$ for the two kinds of collagen model peptides is much smaller than those reported by Kawahara et al.[21] Considering that the difference for the PBS solution was quite close to the Kawahara's results (not shown here), $\bar{v}$ data by Kawahara and our data for PBS could possibly be affected by the effect from the preferential adsorption known for multi-component systems.

Concluding Remarks

In the present study, we have determined the mean-square radius of gyration $<S^2>$, the scattering function $P(k)$, the molar ellipticity $[\theta]$, and the partial specific volume $\bar{v}$ as a function of temperature for four kinds of model peptides (Gly-Hyp-Hyp)$_n$, (Gly-Pro-Hyp)$_n$, (Gly-Hyp-Pro)$_n$, and (Gly-Pro-Pro)$_n$ with different chain length, $n = 5$ and 9, in pure water and 20 mM phosphate buffer containing 150 mM sodium chloride, to clarify why the peptide Ac-(Gly-Hyp-Hyp)$_{10}$-NH$_2$ triple helix having a small transition enthalpy has a higher thermal stability than the peptide Ac-(Gly-Pro-Hyp)$_{10}$-NH$_2$.[25] The results indicate that water plays an important role in the observed differences in the thermodynamic parameters. (Gly-Pro-Hyp)$_9$ shows an increase in hydration upon triple helix formation, whereas (Gly-Hyp-Hyp)$_9$ shows a decrease in hydration. This is consistent with the observed higher transition enthalpy for the former and the observed lower transition entropy for the latter. The net result of these factors is a slightly higher transition temperature for (Gly-Hyp-Hyp)$_9$ [Figure 2(e)]. Hydration between the adjacent Hyp residues of this peptide in the monomeric chain was hypothesized.[27] While we do find an increased hydration of these monomeric chains, this does not lead to an expected stiffening of these structures. The radius of gyration for all molecularly dispersed peptides mostly depends on the number of peptide residues and agrees with chemically denatured proteins irrespective of the amino acid

sequence. This is reasonable, since the Tiffany and Krimm model suggests that unfolded globular proteins contain short stretches of polyproline II-like structures. Therefore, the traditional view, that is, the high content of imino acids in collagens, which restricts the conformational freedom of the monomeric chain, is not sufficient for triple helix formation. Rather, the tendency of the Gly-Pro-Hyp and Gly-Hyp-Hyp sequences to interact with each other in the unfolded state, as shown by the negative second virial coefficient, seems to be important. The Gly-Hyp-Pro peptide shows a positive second virial coefficient at short chain length and peptides with this sequence never form a triple helix.

The increase in the hydration for (Gly-Pro-Hyp)$_9$ upon triple helix formation indicates an important role for water in this structure. However, as our results indicate, a careful analysis of the hydration of the unfolded chains is important, as only a net increase in water binding can add to the stability of the triple helix. Other factors are likely to also play important roles. The *cis/trans* ratio of peptide bonds and the proline ring puckering influence the stability of the triple helix as well. The stability of the collagen triple helix is likely to be based on all of these factors.

References

1. Privalov, P. L. *Adv. Protein. Chem.* **1982**, *35*, 1-104.
2. Gustavson, K. H. *In The chemistry and reactivity of collagen*; Academic Press: New York, 1956.
3. Kobayashi, Y.; Sakai, R.; Kakiuchi, K.; Isemura, T. *Biopolymers* **1970**, *9*, 415-425.
4. Okuyama, K.; Tanaka, N.; Ashida, T.; Kakudo, M.; Sakakibara, S.; Kishida, Y. *J. Mol. Biol.* **1972**, *72*, 571-576.
5. Okuyama, K.; Okuyama, K.; Arnott, S.; Takayanagi, M.; Kakudo, M. *J. Mol. Biol*. **1981**, *152*, 427-443.
6. Hongo, C.; Noguchi, K.; Okuyama, K.; Tanaka, Y.; Nishio, N. *J. Biochem.* **2005**, *138*, 135-144.
7. Okuyama, K.; Xu, X.; Iguchi, M.; Noguchi, K. *Biopolymers* **2006**, *84*, 181-191.
8. Okuyama, K.; Wu, G.; Jiravanichanun, N.; Hongo, C.; Noguchi, K. *Biopolymers* **2006**, *84*, 421-432.
9. Sakakibara, S.; Inoue, K.; Shudo, K.; Kishida, Y.; Kobayashi, Y.; Prockop, D. J. *Biochim. Biophys. Acta* **1973**, *303*, 198-202.
10. Ward, A. R.; Mason, P. *J. Mol. Biol.* **1973**, *79*, 431-435.
11. Jimenez, S.; Harsch, M.; Rosenbloom, J. *Biochem. Biophys. Res. Commun.* **1973**, *52*, 106-114.
12. Berg, R. A.; Prockop, D. J. *Biochem. Biophys. Res. Commun.* **1973**, *52*, 115-120.
13. Engel, J.; Chen, H. T.; Prockop, D. J. *Biopolymers* **1977**, *16*, 601-622.
14. Fields, G. B.; Prockop, D. J. *Biopolymers* **1996**, *40*, 345-357.
15. Bella, J.; Brodsky, B.; Berman, H. M. *Structure* **1995**, *3*, 893-906.
16. Okuyama, K.; Hongo, C.; Fukushima, R.; Wu, G.; Narita, H.; Noguchi, K.; Tanaka, Y.; Nishio, N. *Biopolymers* **2004**, *76*, 367-377.
17. Mizuno, K.; Hayashi, T.; Peyton, D. H.; and Bächinger, H. P. *J. Biol. Chem*. **2004**, *279*, 282-287.
18. Nishi, Y.; Uchiyama, S.; Doi, M.; Nishiuchi, Y.; Nakazawa, T.; Ohkubo, T.; Kobayashi, Y. *Biochemistry* **2005**, *44*, 6034-6042.
19. Raines, R. T. *Protein Sci.* **2006**, *15*, 1219-1225.

20.   Melacini, G.; Bonvin, A. M. J. J.; Goodman, M.; Boelens, R.; Kaptein R. *J Mol Biol.* **2006**, *300*, 1041-1048.

21.   Kawahara, K.; Nishi, Y.; Nakamura, S.; Uchiyama, S.; Nishiuchi, Y.; Nakazawa, T.; Ohkubo, T.; Kobayashi, Y. *Biochemistry* **2005**, *44*, 15812-15822.

22.   DeRider, M. L.; Wilkens, S. J.; Waddell, M. J.; Bretscher, L. E.; Weinhold, F.; Raines, R. T.; Markley, J. L. *J. Am. Chem. Soc*. **2002**, *124*, 2497-2505.

23.   Vitagliano, L.; Berisio, R.; Mazzarella, L.; Zagari, A. *Biopolymers* **2001**, *58*, 459-464.

24.   Bretscher, L. E.; Jenkins, C. L.; Taylor, K. M.; DeRider, M. L.; Raines, R. T. *J. Am. Chem. Soc.* **2001**, *124*, 2497-2505.

25.   Mizuno, K.; Hayashi, T.; Peyton, D. H.; Bächinger, H. P. *J. Biol. Chem.* **2004**, *279*, 38072-38078.

26.   Doi, M.; Nishi, Y.; Uchiyama, S.; Nishiuchi, Y.; Nishio, H.; Nakazawa, T.; Ohkubo, T.; Kobayashi, Y. *J. Peptide Sci*. **2005**, *11*, 609-616.

27.   Schumacher, M.; Mizuno, K.; Bächinger, H. P. *J. Biol. Chem*. **2005**, *280*, 20397-20403.

28.   Berry, G. C. *J. Chem. Phys.* **1966**, *44*, 4550-4564.

29.   Glatter, O.; Kratky, O. *Small Angle X-ray Scattering*; Academic Press: London, 1982.

30.   Holtzer, A. *J. Polym. Sci.* **1955**, *17*, 432-434.

31.   Pedersen, J. S.; Schurtenberger, P. *J. Appl. Crystallogr.* **1996**, *29*, 646-661.

32.   Nakamura, Y.; Norisuye, T. *J. Polym. Sci. B: Polym. Phys.* **2004**, *42*, 1398-1407.

33.   Svergun, D.; Barberato, C.; Koch, M. H. J. *J. Appl. Crystallogr.* **1995**, *28*, 768-773.

34.   Kohn, J. E.; Millett, I. S.; Jacob, J.; Zagrovic, B.; Dillon, T. M.; Cingel, N.; Dothager, R. S.; Seifert, S.; Thiyagarajan, P.; Sosnick, T. R.; Hasan, M. Z.; Pande, V. S.; Ruczinski, I.; Doniach, S.; Plaxco, K. W. *Proc. Natl. Acad. Sci. U. S. A.* **2004**, *101*, 12491-12496.

35.   Tiffany M. L.; Krimm S. *Biopolymers* **1968**, *6*, 1379-1382.

36.   Creamer T. P.; Campbell M. N. *Adv. Protein. Chem*. **2002**, *62*, 263-282.

37.   Zagrovic, B.; Lipfert, J.; Sorin, E. J.; Millett, I. S.; Gunsteren, W. F.; Doniash, S.; Pande, V. S. *Proc. Natl. Acad. Sci. U. S. A*. **2005**, *102*, 11698-11703.

38.   Hickl, P.; Ballauff, M.; Scherf, U.; Müllen, K.; Lindner, P. *Macromolecules* **1997**, *30*, 273-279.

39.   Benoit, H.; Doty, P. *J. Phys. Chem.* **1953**, *57*, 958-963.

40.   Konishi, T.; Yoshizaki, T.; Saito, T.; Einaga, Y.; Yamakawa, H. *Macromolecules* **1990**, *23*, 290-297.

41.   Clark, D. S.; Mattice, W. L. *Macromolecules* **1977**, *10*, 369-374.

Table 1. Results from SAXS Measurements of Collagen Model Peptides in Pure Water.

Sample	Temperature (°C)	M [a]	M_w	A_2 (10^{-3} mol cm^3 g^{-2})	$<S^2>^{1/2}$ (nm)
(Gly-Hyp-Hyp)$_9$	15	2567	7750	1.0	2.30
	70		–	–	1.55
(Gly-Pro-Hyp)$_9$	15	2424	7800	0.9	2.27
	70		–	–	1.52
(Gly-Hyp-Hyp)$_5$	15	1434	1440 [b]	−1.3	1.10
	70		–	–	1.03
(Gly-Pro-Hyp)$_5$	15	1354	1350 [b]	−0.8	1.06
	70		–	–	1.01
(Gly-Hyp-Pro)$_5$	15	1354	–	1.4	1.05

[a] Calculated molecular weight for single chain, [b] leading to the mean of the calibration constant K for SAXS measurements.

Table 2. Results from SAXS Measurements of Collagen Model Peptides in PBS (20 mM Phosphate Buffer Containing 150 mM NaCl).

Sample	Temperature (°C)	A_2 (10^{-3} mol cm^3 g^{-2})	$<S^2>^{1/2}$ (nm)
(Gly-Hyp-Hyp)$_9$	15	0.5	2.40
	75	0.8	1.53
(Gly-Pro-Hyp)$_9$	15	0.7	2.43
	75	1.2	1.51
(Gly-Hyp-Hyp)$_5$	15	−1.7	1.09
	75	2.2	1.04
(Gly-Pro-Hyp)$_5$	15	−1.8	1.05
	75	2.5	1.02
(Gly-Hyp-Pro)$_9$	75	1.8	1.52
(Gly-Hyp-Pro)$_5$	75	2.5	1.01
(Gly-Pro-Pro)$_9$	75	0.8	1.47
(Gly-Pro-Pro)$_5$	75	1.7	0.99

Chart 1.
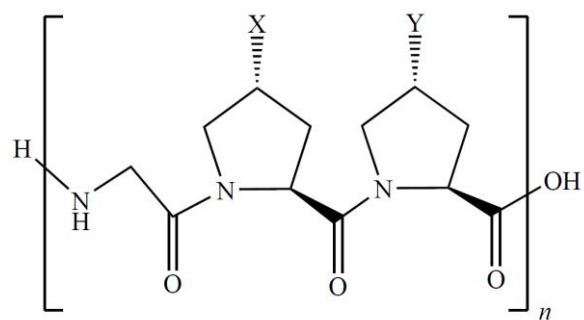
1. H-(Gly-4(*R*)Hyp-4(*R*)Hyp)$_n$-OH: X = OH, Y = OH
2. H-(Gly-Pro-4(*R*)Hyp)$_n$-OH: X = H, Y = OH
3. H-(Gly-4(*R*)Hyp-Pro)$_n$-OH: X = OH, Y = H
4. H-(Gly-Pro-Pro)$_n$-OH: X = H, Y = H

FIGURE CAPTIONS

Figure 1. Circular dichroism spectra of (a) H-(Gly-Hyp-Hyp)$_9$-OH, (b) H-(Gly-Pro-Hyp)$_9$-OH, (c) H-(Gly-Hyp-Pro)$_9$-OH, and (d) H-(Gly-Pro-Pro)$_9$-OH in PBS at indicated temperatures. Peptide concentration, $(1-3)\times10^{-4}$ g cm^{-3}.

Figure 2. Temperature dependence of $[\theta]$ for (a) H-(Gly-Hyp-Hyp)$_n$-OH, (b) H-(Gly-Pro-Hyp)$_n$-OH, (c) H-(Gly-Hyp-Pro)$_n$-OH, and (d) H-(Gly-Pro-Pro)$_n$-OH in pure water (triangles) and in PBS (circles) at the wavelength of 225 nm. Peptide concentration, $(1-3)\times10^{-4}$ g cm^{-3}. Open and filled symbols indicate $n = 5$ and 9, respectively. (e) High peptide concentration $(3.9\times10^{-3}$ g cm$^{-3})$ data for H-(Gly-Hyp-Hyp)$_9$-OH (open square) and H-(Gly-Pro-Hyp)$_9$-OH (filled square) in water.

Figure 3. Berry plots for (a) H-(Gly-Hyp-Hyp)$_9$-OH and (b) H-(Gly-Hyp-Hyp)$_5$-OH in pure water at 15 °C. For clarity, the ordinate values of $(c/\Delta I_\theta)^{1/2}$ are shifted by arbitrary constants (A) indicated in parentheses.

Figure 4. Concentration dependence of M_{app} for (a) H-(Gly-Hyp-Hyp)$_n$-OH and (b) H-(Gly-Pro-Hyp)$_n$-OH, both in pure water. Open and filled symbols indicate $n = 5$ and 9, respectively.

Figure 5. Temperature dependence of A_2 for collagen-model peptides forming triple helical structure (triangles) and dispersing in solution as a single molecule (circles) in pure water (filled symbols) and in PBS (open symbols).

Figure 6. $<S^2>^{1/2}$ for the collagen-model peptides in pure water and in PBS at 15, 70, and 75 °C plotted against the number of residues. Triangles, peptides forming triple helical structure; circles, peptides dispersing in solution as a single molecule; crosses, literature data for chemically denatured proteins [ref 34].

Figure 7. Holtzer plots for H-(Gly-Pro-Hyp)$_9$-OH (open triangles) and H-(Gly-Hyp-Hyp)$_n$-OH (filled triangles) in PBS at 15 °C. Solid curves, theoretical values for straight cylinders calculated from eq 5 with the indicated parameters. Dashed curve, values for the crystal structure computed by CRYSOL [ref 33] using the coordinates of the modified 1YM8 (see text). The ordinate values of $kP(k)$ are shifted by A.

Figure 8. Cross-sectional plots for H-(Gly-Pro-Pro)$_n$-OH (open circles), H-(Gly-Hyp-Pro)$_n$-OH (filled circles), H-(Gly-Pro-Hyp)$_n$-OH (open triangles), and H-(Gly-Hyp-Hyp)$_n$-OH (filled triangles) in PBS at 75 °C. (a) H-(Gly-X-Y)$_9$-OH, (b) H-(Gly-X-Y)$_5$-OH. The ordinate values of $\ln(kP(k))$ are shifted by A.

Figure 9. Holtzer plots for H-(Gly-Pro-Pro)$_n$-OH (open circles), H-(Gly-Hyp-Pro)$_n$-OH (filled circles), H-(Gly-Pro-Hyp)$_n$-OH (open triangles), and H-(Gly-Hyp-Hyp)$_n$-OH (filled triangles) in PBS at 75 °C. Curves, Nakamura-Norisuye's theoretical values for the wormlike cylinder with the common h and λ^{-1} of 0.33 and 2 nm, respectively, and d of 0, 0.45, 0.45, and 0.67 nm from top to bottom in each panel.

Figure 10. Temperature dependence of $\bar{v}$ (a) and the ratio $\bar{v}_T/\bar{v}_{75°C}$ (b) for H-(Gly-Pro-Hyp)$_5$-OH (open triangles), H-(Gly-Pro-Hyp)$_9$-OH (filled triangles), H-(Gly-Hyp-Hyp)$_5$-OH (open circles), and H-(Gly-Hyp-Hyp)$_9$-OH (filled circles) in pure water. Large and small symbols are obtained from independent measurements.
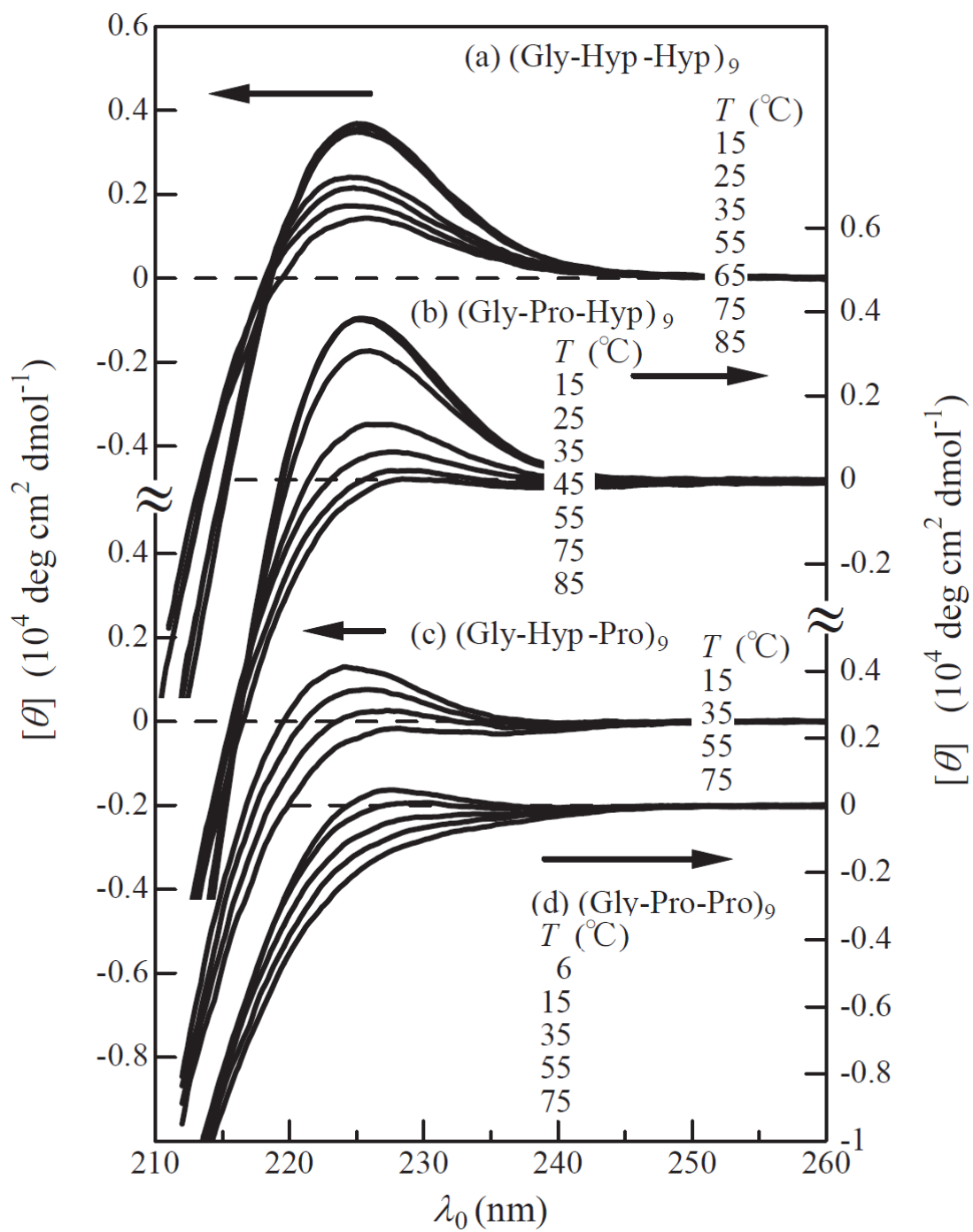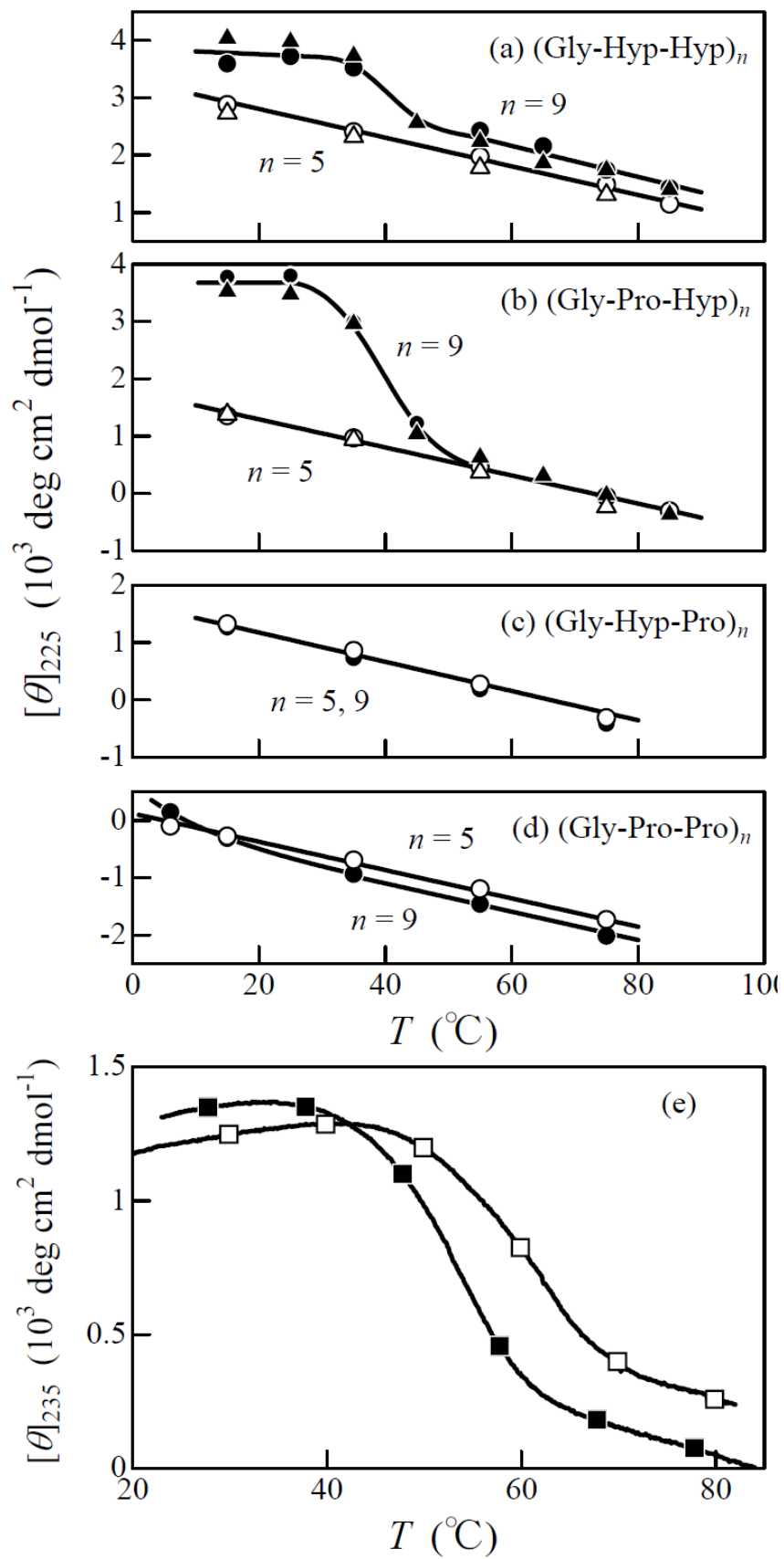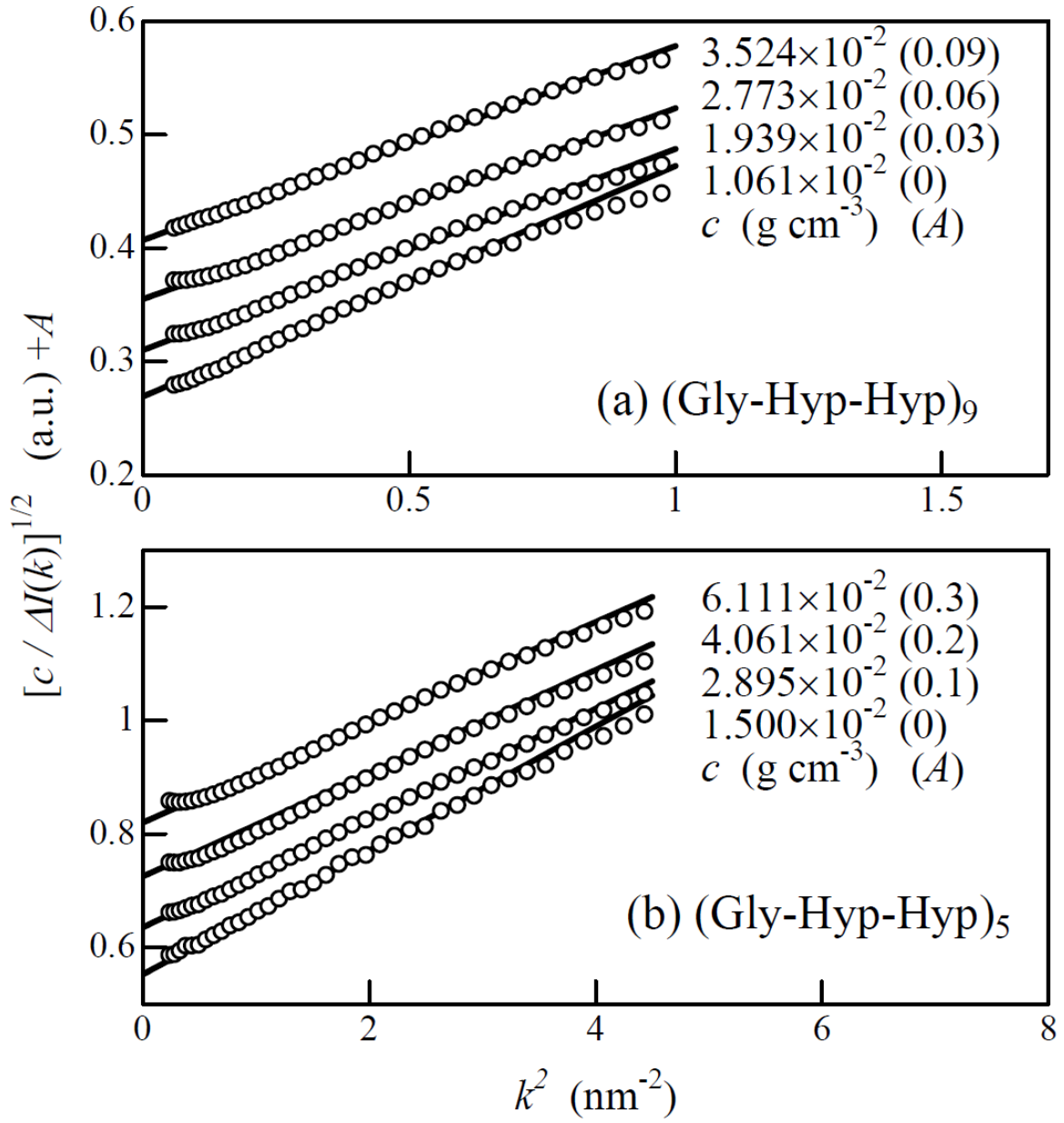
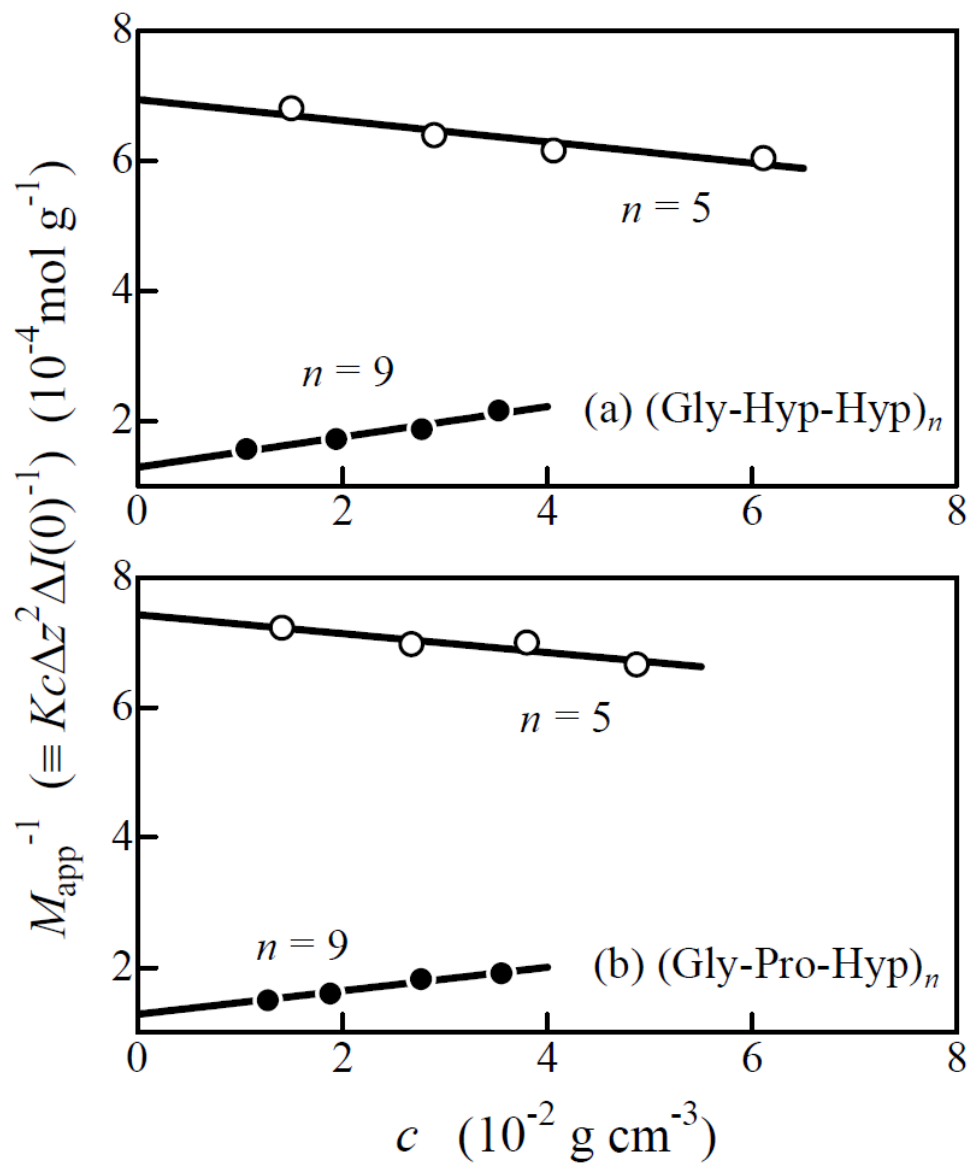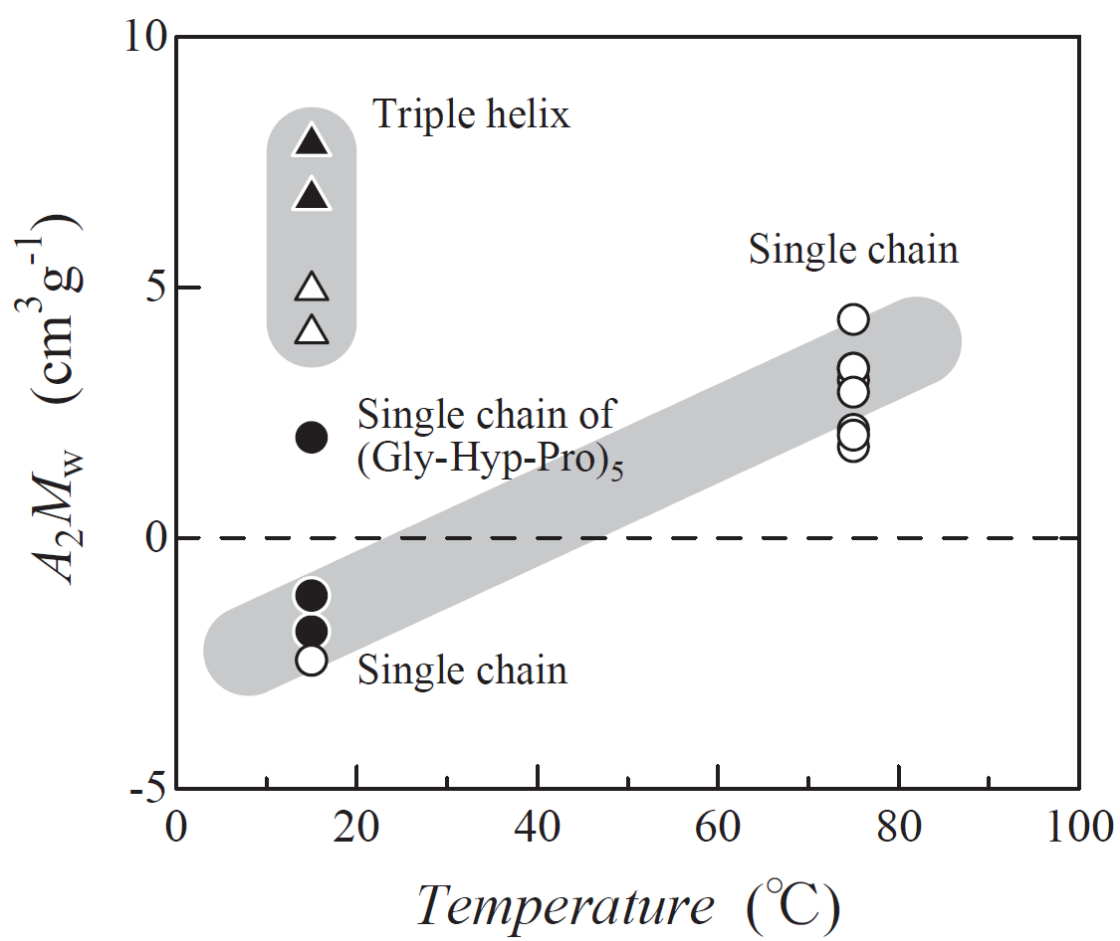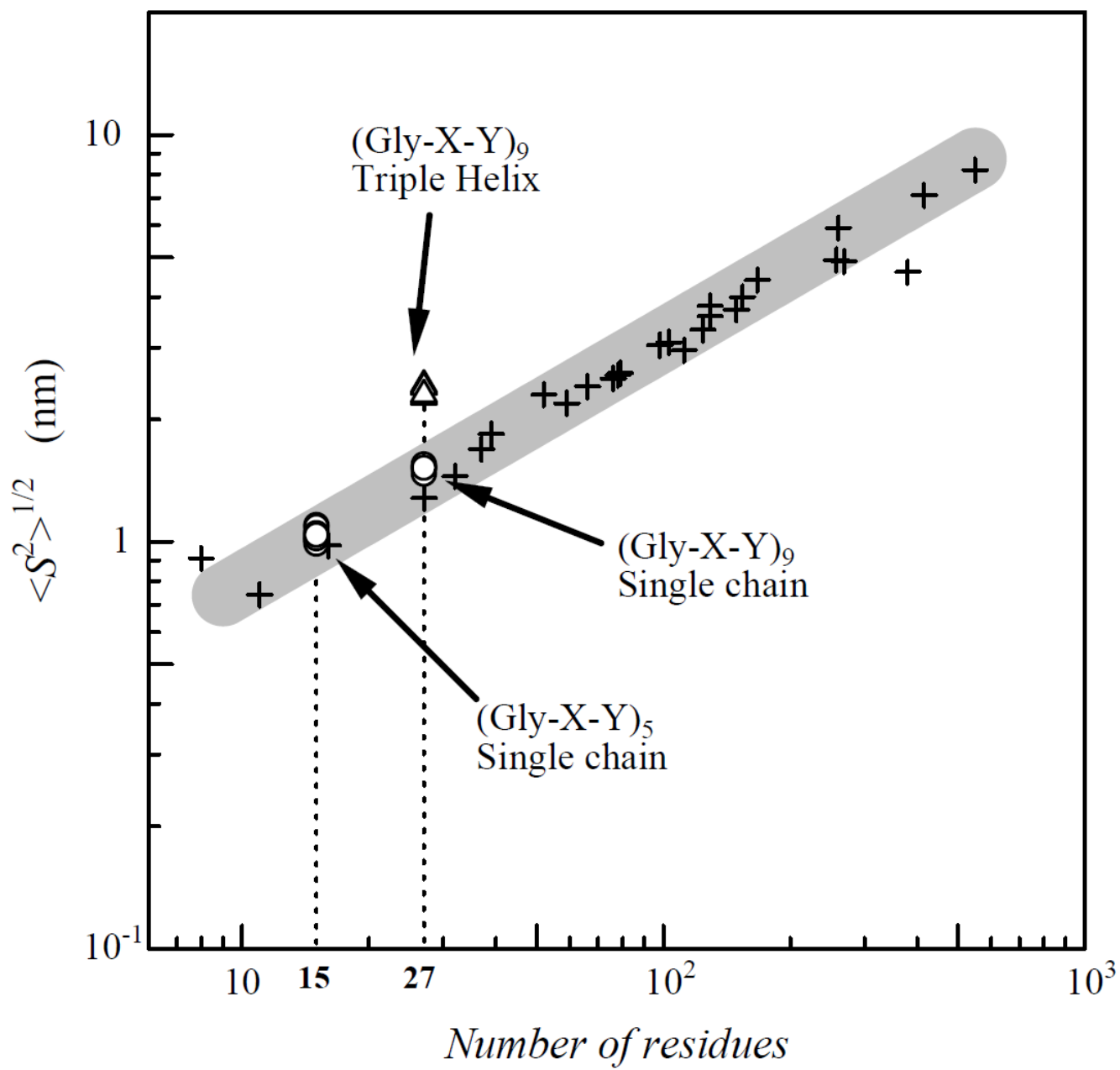**Figure 1.**

Figure 2.

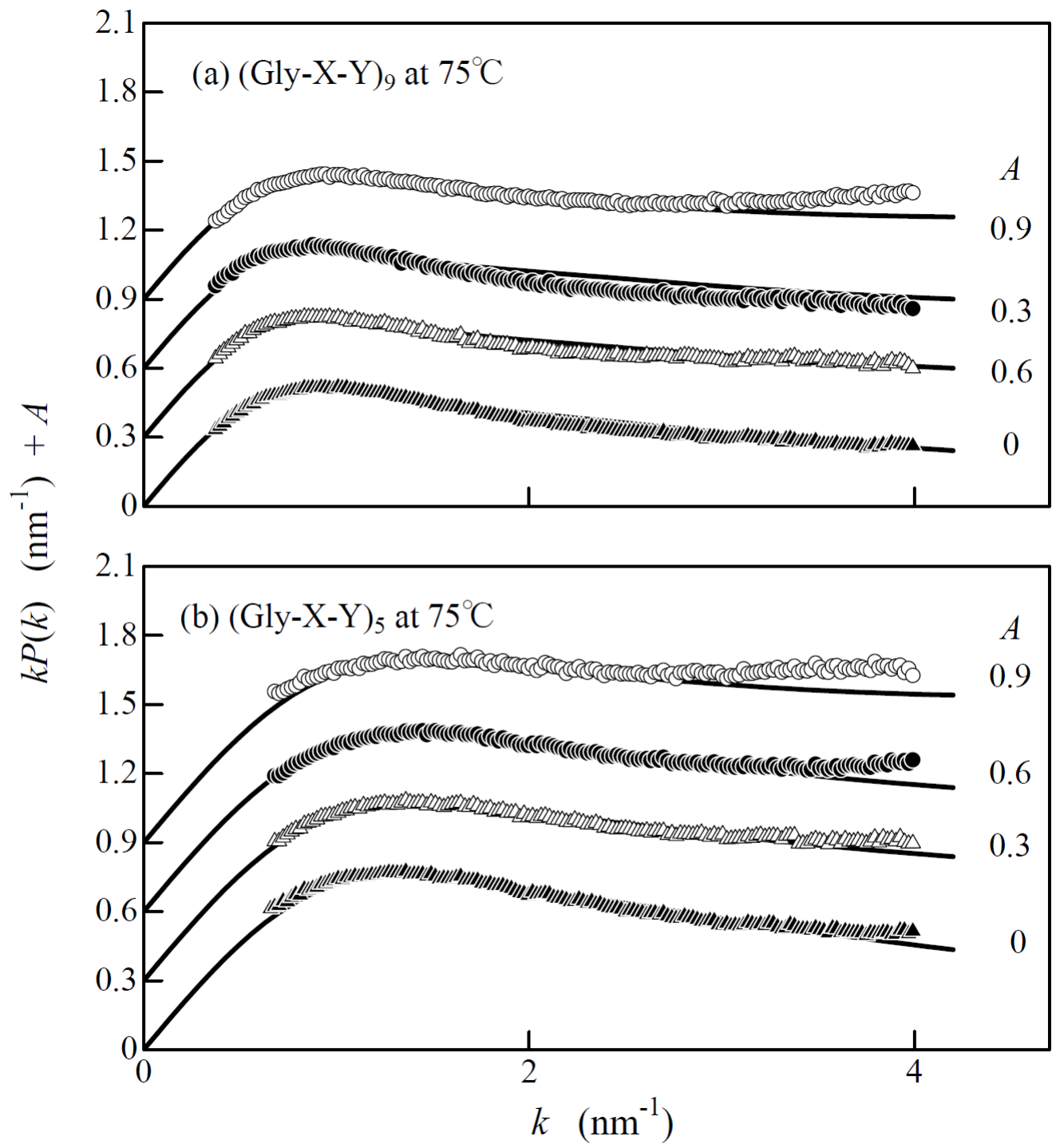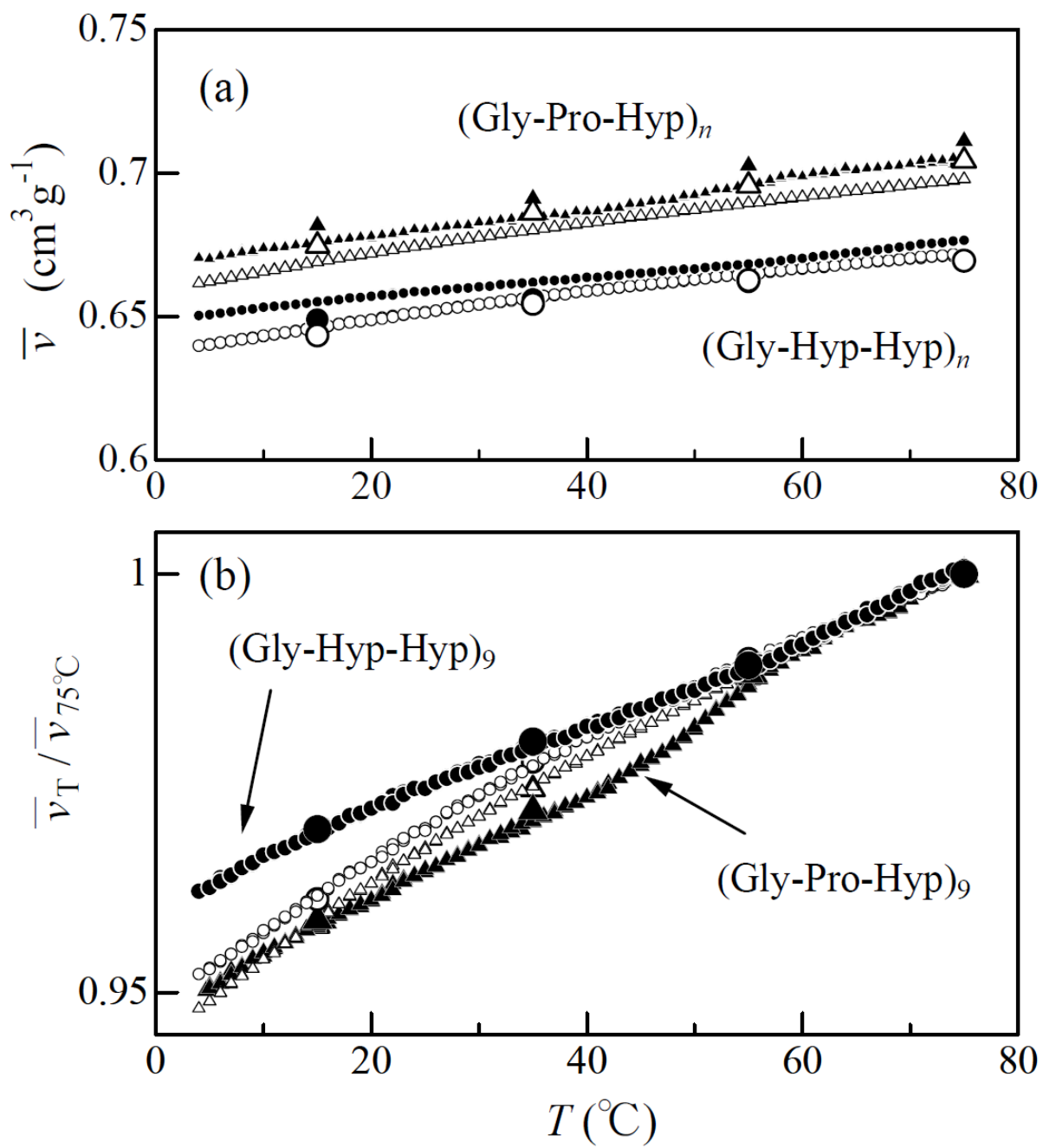**Figure 3.**

Figure 4.

Figure 5.

Figure 6.
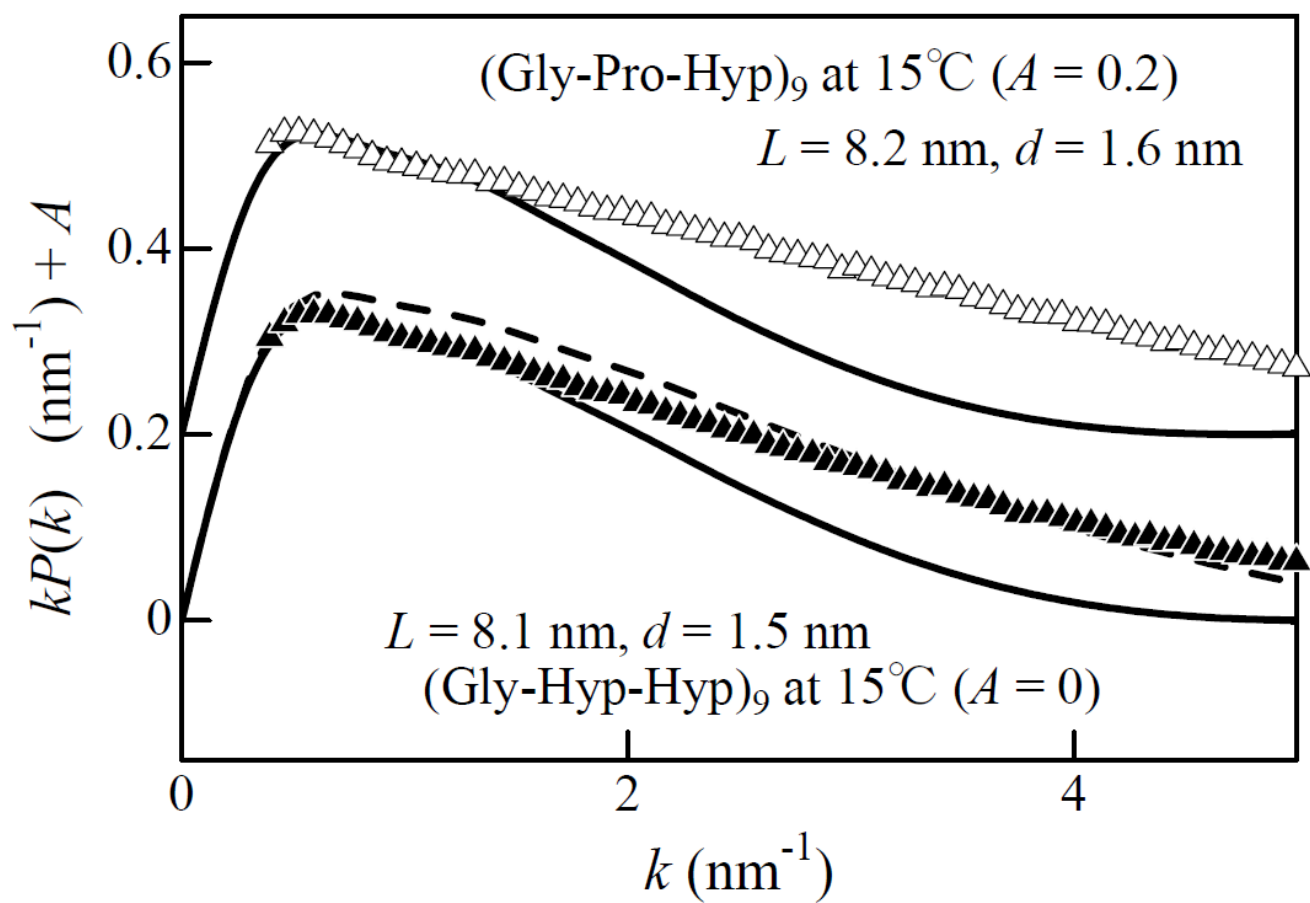
Figure 7.
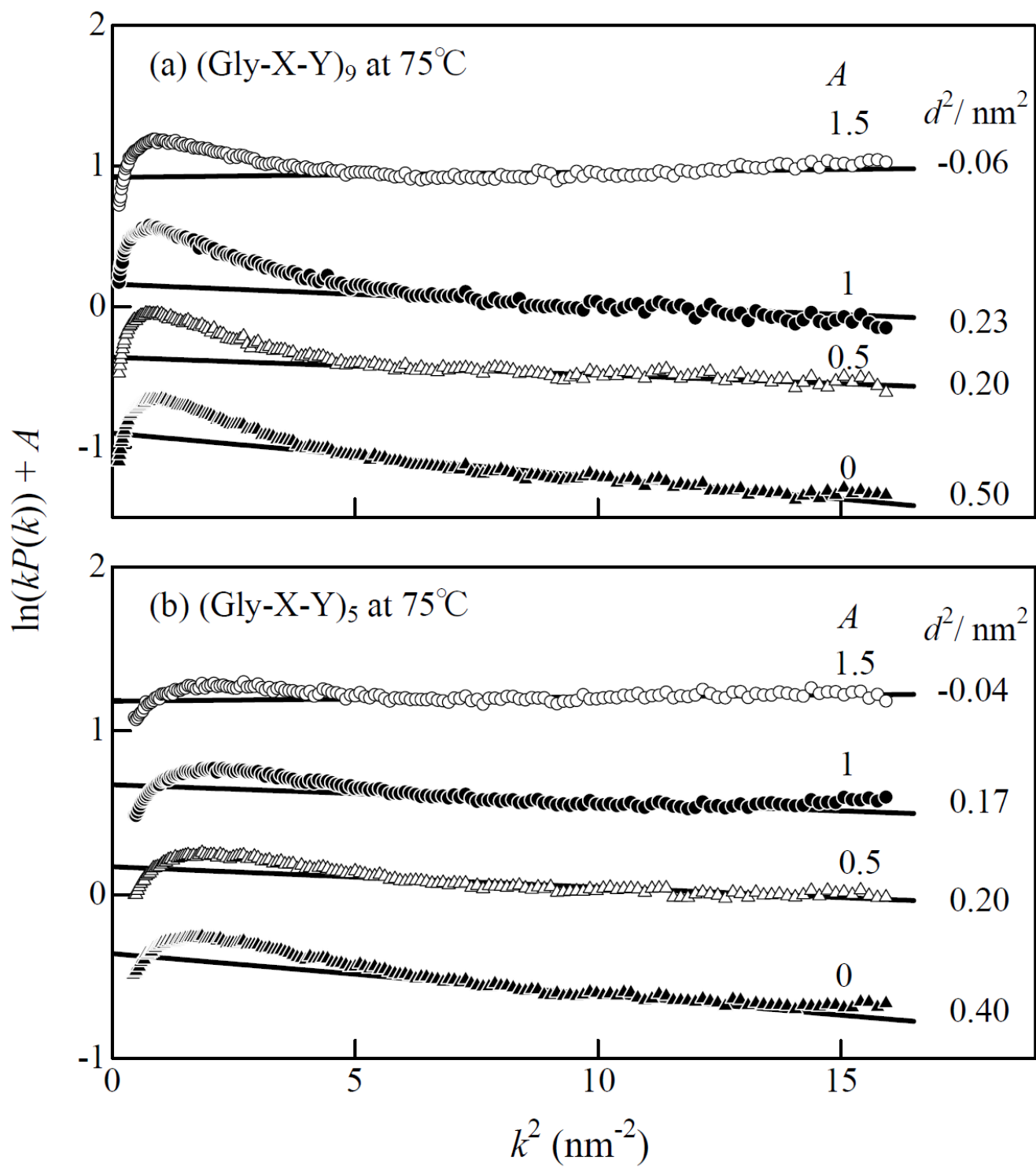
Figure 8.

Figure 9.

Figure 10

Table of Contents